Aerobiologia
DOI 10.1007/s10453-014-9345-3

ORIGINAL PAPER

A comparative study of vineyard phenology and pollen metrics extracted from airborne pollen time series

Mário Cunha · Helena Ribeiro · Paulo Costa · Ilda Abreu

Received: 13 March 2014 / Accepted: 12 June 2014

Abstract Airborne pollen emission model was used to determine pollen metrics and to examine their relationship with vineyard phenology in two wine regions of Northern Portugal: Vinhos Verdes (1993–2007) and Douro (1992–2011). A number of airborne pollen metrics were obtained through the rate of changes of logistic model adjusted to the time series of airborne pollen. In both regions, the mean absolute differences between observed phenology and model-predicted values for start, peak and final of flowering phenophases were always lower than 5 days and the slope of the regression through the origin is close to one. These metrics can be used to accurately and precisely predict the dynamic of *Vitis* flowering observed at field level. The model's simplicity and flexibility are of great advantage for its practical use in aerobiology.

Keywords Pollen emission model · Airborne pollen metrics · Pollen season · Grapevine · Phenology · Crop yield forecast

M. Cunha (✉) · I. Abreu
Faculdade de Ciências, Universidade do Porto, Rua do Campo Alegre, s/n, 4169-007 Porto, Portugal
e-mail: mcunha@mail.icav.up.pt

M. Cunha
Centro de Investigação em Ciências Geo-espaciais, Rua do Campo Alegre, s/n, 4169-007 Porto, Portugal

H. Ribeiro · I. Abreu
Centro de Geologia da Universidade do Porto, Rua do Campo Alegre, s/n, 4169-007 Porto, Portugal

P. Costa
Associação para o Desenvolvimento da Viticultura Duriense (ADVID), Quinta de Sta. Maria Apartado 137, 5050-106 Godim (Peso da Régua), Portugal

1 Introduction

Metrics based on airborne pollen time series give important information as support for a variety of scientific and technological studies and abiotic processes. These pollen metrics have been further classified as pollen quantity indices (e.g. annual or season production and peak value) and pollen timing indices like start, peak and end dates of pollen season. The terminology, determination and interpretation of the pollen metrics and their use are often discussed, and reviews can be found in several scientific articles (e.g. Helbig et al. 2004; Driessen et al. 1989).

The pollen metrics are closely associated with several aerobiological applications such as allergic airway diseases (e.g. Weger et al. 2013), land cover change (e.g. Emberlin et al. 2000), crop yield forecast (e.g. Cunha et al. 2003), conservation of biodiversity (e.g. Kuparinen et al. 2007; Fernández-Llamazares et al. 2013a) and, more recently, for assessment of the impact of climate change on vegetation dynamic (e.g. Cristofori et al. 2010; Fernández-Llamazares et al.

Published online: 22 June 2014

2013b). The determination of metrics related to the main pollen season is also important to estimate the quantity of pollen coming effectively from the studied region avoiding pollen deposition and recirculation (e.g. Charalampopoulos et al. 2013) as well as the transported pollen from long distances (Fernández-Llamazares et al. 2013a; Estrella et al. 2006). The accurate estimation of the quantity of pollen that, effectively, comes from a determined region is particularly important for early-season estimate of crop production based on airborne pollen samples (Cunha et al. 2003; Orlandi et al. 2005).

Airborne pollen time series pattern is well known to depend on the dynamic of flowering phenophase of the surrounding vegetation (Estrella et al. 2006; Kasprzyk and Walanus 2010; Siljamo et al. 2008a; Jato et al. 2007) and the intricate effect of climate on the airborne pollen dispersion and deposition (Zhang et al. 2013; Duhl et al. 2013; Scheifinger et al. 2013). However, an open question is how sensitive are these relationships to seasonal and interannual phenology variability. It is known that pollen resuspension processes, including the rebound and the re-entrainment of pollen after deposition to the ground or on plant surface, can contribute to increased airborne pollen concentration (Jarosz et al. 2004; Helbig et al. 2004). Also, pollen coming from other regions can have a significant impact on the pollen index as well as on the increase of the length of the pollen season (Kasprzyk 2003; Rousseau et al. 2003; Cambon et al. 1992). The contribution of the pollen provided by resuspension process and long-range transport is particularly important during the start and final of the flowering season and can be mitigated by the use of only a period of the whole pollen season.

Faced with these possibilities, it is necessary to know to what temporal extent local pollen production (defined by field observations) is not the source of pollen found on the neighbouring traps. During the last 40 years, several approaches have been proposed for detecting temporal changes and extract metrics from airborne pollen time series that can be related to surrounding vegetation dynamic, for example, using daily or accumulated daily sum of pollen concentration reaching a particular threshold (Giorato et al. 2000; Sánchez Mesa et al. 2003; Feher and JaraiKomlodi 1997; Davies and Smith 1973), when the accumulated sum reaching one percentage of the total annual pollen (Helbig et al. 2004; Nilsson and Persson 1981; Andersen 1991; Galán et al. 1995; Lejoly-Gabriel and Leuschner 1983; Torben 1991; Mullenders et al. 1972; Spieksma et al. 1995) or with the aid of plants flowering earlier—indicator plants (Driessen et al. 1989). Other methods, based on computational intelligence methods (Scheifinger et al. 2013) or on temporal trajectory analysis of modelled airborne time series (Cunha et al. 2003; Pathirane 1975; Kasprzyk and Walanus 2010; Ruffaldi and Greffier 1991), have been proposed for smoothing and detecting temporal changes and respective metrics to the values of pollen.

Reviews of the merits and limitations of these techniques can be found in scientific articles (Helbig et al. 2004; Cunha et al. 2003; Driessen et al. 1989; Scheifinger et al. 2013). According to these publications, the drawback of defining the pollen metrics during the season using a fixed threshold value may imply that the season does not start at all in years with very low airborne pollen concentration and, the percentage method cannot be used until the end of season. Moreover, both criteria are specific for each *taxon* and depend on start date used for pollen counts. The indicator plants are used only for the start of the pollen season on behalf of allergic airway diseases. The present methods based on trajectory analysis need complementary complicate and tedious tests (e.g. sensitive tests, specific threshold or change trajectories) to extract the metrics from airborne time series. Moreover, only few of these methods were tested against observed phenological data in long-term studies. The restrictions of existing approaches can make the modelling of airborne pollen flows to extract metrics that could be related to the surrounding vegetation flowering phenophase challenging.

In this work, we are therefore engaged to identify the linkages between airborne pollen metrics and field observations of flowering dynamic using long time series of monitored data. The following question was addressed in this study: Is there any mathematical model adjustable to the temporal airborne pollen flows from different years and regions that can be able to explain the season and interannual variability of flowering dynamic observed at field? The results from previous works show that a logistic regression model fits well the airborne pollen results of the serial filters exposed during the *Vitis* flowering period (Cunha et al. 2003) in several regions of Portugal and Pinaceae, Poaceae, Urticaceae, *Acer*, *Platanus*, *Castanea*, Cupressaceae, *Alnus*, and *Fraxinus* (Ribeiro et al. 2007)

Fig. 1 Location of the airborne pollen traps (*black circle*), climatic characteristics and vineyard phenology

Location and sampler Parameters	Vinhos Verdes Region	Douro Region
Location of pollen traps	Amarante	Peso da Régua
Latitude; Longitude	41°16´N 8°05´W	41°10´N; 7°48´W
Altitude (a.b.s.) (m)	110	65
Height of pollen trap (m)	12	19
Airborne sampling period	1993 – 2007	1992 – 2011
Vineyard phenology data[a]	SF, MF and FF	MF and FF
Main grapes varieties	White: Loureiro, Trajadura and Pedernã	Red: Touriga Franca, Tinta Roriz and Barroca
Vineyard surface (ha)	21540	38235
Vineyard surface (%)[b]	15.1	26.8
Annual av. temperature (ºC)	13 – 16	12 – 15
Annual rainfall (mm)	1129	856
Summer AWR (%)[c]	22 – 55	<20
Climatic classification[d]	$B_4B'_2s_1$ a'	$B_1B'_2s_2$ a'

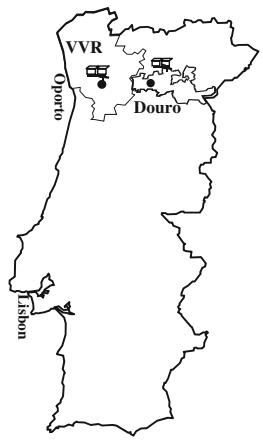

[a]SF: Start of Flowering; MF: Main Flowering; FF: Final Flowering.
[b]relatively to the total of Portugal (region/Portugal x 100)
[c]Available Water Reserve (AWR), in the first 10 days of September (end of the ripening phase).
[d]According to Thornthwaite Climatic Classification. Hydric index: B_1 (little humid) and B_4 (very humid). Thermal efficiency index: B'_2 (mesotermic). Aridity index: Shortage of water in summer: s (moderate); r (null or small). Thermal efficiency summer concentration index: a'>20%, typically continental.

in north of Portugal (Oporto) and Olea (Ribeiro et al. 2009) in the south of Portugal (Alentejo).

The overall goal of this paper was to analyse the spatial and temporal coherence between locally observed flowering dates and the ones derived from airborne pollen counts. Although the causal relationship between the dynamic of flowering phenophase seems to be evident, there is a great lack of knowledge in this field.

For this study, we chose a long-time dataset of phenological observations and airborne pollen counts of *Vitis* used mainly for regional wine production forecast in two Portuguese main wine regions: Vinhos Verdes and Douro (Cunha et al. 2003).

2 Materials and methods

2.1 Studied area

The research was carried out in two main wine regions of northern Portugal: Vinhos Verdes region (VVR; 1993–2007) and Douro (1992–2011). The VVR is located in an area traditionally known as Entre-Douro-e-Minho. The mountainous areas in the East and South, forming the natural border between the Atlantic Entre-Douro-e-Minho and the Mediterranean inland regions, belong to the Douro region (Fig. 1).

These regions differ greatly in terms of weather, soils, grape variety, vine-growing systems, crop-growing techniques, impact of diseases on crop size and wine yield. In the Douro region red grape varieties predominate, while in VVR the most frequent varieties are the white ones (Fig. 1).

Grapevines grown in VVR have unique characteristics, namely the form of guiding systems with wide vegetative expansion and growth high above the ground. In Douro, also known as the Port wine region, vineyards are in stony soils and the large majority planted in hillsides with steep slopes. Also, mostly in the eastern part in this region, the vineyards are located in some of the most arid regions of Europe.

According to Köppen's classification, both regions belong to the group Csb (temperate, with dry summer, which is not very hot but extensive), while Thornthwaite's rational climate classification presents different climatic indices for the studied regions (Fig. 1).

In both regions, the most significant climatic feature is an irregular annual rainfall level distributed throughout the year, mainly concentrated in winter and spring. Air temperature increases inversely to precipitation: winters are cool and wet, and hot and dry summers.

2.2 Vineyard phenology and airborne pollen sampling

The grapevine phenology observations were collected in a field located at 6 km (VVR) and 5 km (Douro) from the respective Cour trap. The grapevine

phenology was performed according to the *Baggiollini* stage scale (Baggiolini 1952). The data were obtained by observations at field levels each 3 days and registered according to the "Organisation Internationale de la vigne et du vin" (OIV) phenophase descriptors (OIV 2009). A given phenological stage was reached, and date recorded when the event occurred in 50 % of the plants in each set. In our study, only the flowering phenophase was studied as follows:

- SF: Start of flowering period (about 10 % of the flowers open)
- MF: Main flowering period (50 % of the flowers open)
- FF: Final flowering period (90 % of the flowers)

The timing of each phenological stage was averaged for the main varieties presented in Fig. 1. For the Douro region, we do not have the start of flowering period and phenological observations for 2010.

Airborne pollen was sampled using one Cour trap for each region. Their location was selected according to the average wind direction during the flowering period (Cunha et al. 2003). In the Cour technique, pollen grains are trapped on gauze filters (400 cm^2) fixed vertically on a wind vane, which continually orientates the filters according to the wind direction (Cour 1974). During flowering, filters were exposed for 3 or 4 days. Airborne pollen flow (APF), obtained by the pollen captured in each filter exposed for 3 or 4 days, was expressed in number of average daily pollen grains transported per square metre of filter (pollen m^{-2}).

After exposure, the pollen grains were removed from the filters using several chemical treatments including the destruction of the gauze, acetolysis and the addition of glycerol for sediment quantification. The identification and pollen count was carried out, independently of the pollen grain concentration, with ten regular traverse rows using an optical microscopic (×630).

2.3 Pollen emission model and airborne pollen metrics

A logistic regression model was fitted annually to the values of the accumulated pollen during the *Vitis* flowering period:

$$y_t = \alpha\left[1+\exp^{-(\beta+\gamma x_t)}\right]^{-1}+e_t; \quad t=1,\ldots,n \tag{1}$$

where y_t is the amount of accumulated pollen up to day x_t referred to the DOY; α is the distance between the two asymptotes, representing the value for which the pollen emission is stabilised; β is a position parameter; γ is the parameter related to the rate of pollen increase; e_t is the random model component; and t is the natural number representing the ordinal of observations. The logistic model has an inflexion point with abscise $x_t = \frac{\hat{\beta}}{\hat{\gamma}}$.

The parameters of the logistic model were estimated by the Levenberg–Marquardt algorithm that requires some reasonable initial values.

The logistic function (1) and its second- to fourth-order derivatives were considered to obtain the airborne pollen metrics:

$$\frac{\delta^2 y}{\delta x^2} = \alpha\gamma^2\exp(-\beta-\gamma x)\times[\exp(-\beta-\gamma x)-1] \times[1+\exp(-\beta-\gamma x)]^{-3} \tag{2}$$

$$\frac{\delta^3 y}{\delta x^3} = \alpha\gamma^3\exp(-\beta-\gamma x) \times\left[1-4\exp(-\beta-\gamma x)+(\exp(-\beta-\gamma x))^2\right] \times[1+\exp(-\beta-\gamma x)]^{-4} \tag{3}$$

$$\frac{\delta^4 y}{\delta x^4} = \alpha\gamma^4\exp(-\beta-\gamma x) \times\left[-1+11\exp(-\beta-\gamma x)-11(\exp(-\beta-\gamma x))^2 +\exp(-\beta-\gamma x)^3\right]\times[1+\exp(-\beta-\gamma x)]^{-5} \tag{4}$$

where the parameters $\alpha > 0$ and $\gamma > 0$.

Figure 2 presents the logistic function and its second- to fourth-order derivatives with the example for Douro region in 2001.

The second derivative of the logistic function represents the acceleration of the process and could be related to the rate of pollen emission. The third and fourth derivative of the logistic function, although do not account for the biophysical process, help to define the pollen metrics.

In both regions, a number of airborne pollen metrics were obtained for each year that correspond to dates in which the rate of change in curvature of

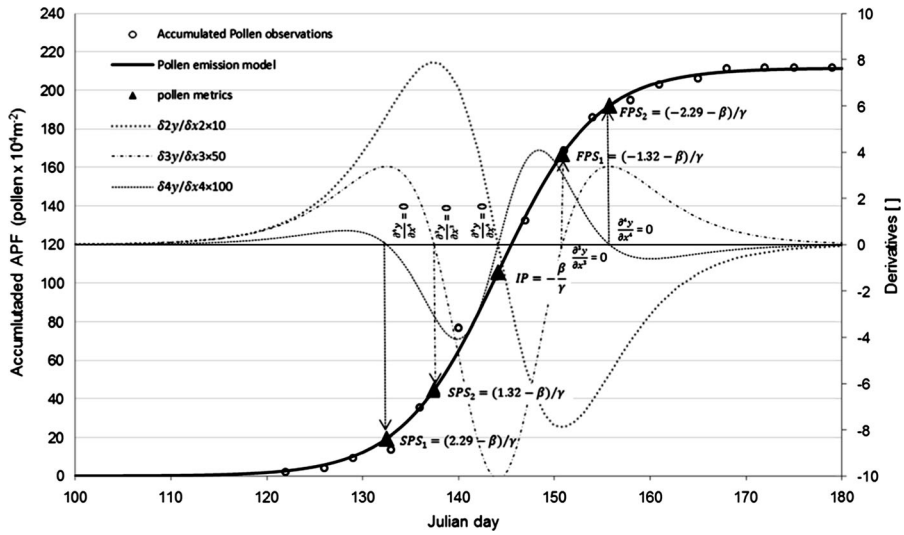

Fig. 2 Accumulated pollen observations, estimated by the logistic model and the second- to fourth-order derivatives for the year 2001 in Douro region. The logistic model parameters for 2001 are as follows: $\alpha = 211.6$; $\beta = -28.4$; and $\gamma = 0.197$. For the figure-scale adjustment, the values of the second- to fourth-order derivatives were magnified by 10, 50 and 100 times, respectively

Table 1 Airborne pollen metrics extracted from the logistic model

Derivatives	Abscissas (x_t values)	Second derivatives function point	Airborne pollen metrics
$\frac{\delta^3 y}{\delta x^3} = 0 \Rightarrow$ $-1 - 4\exp(-\beta - \gamma x) + (\exp(-\beta - \gamma x))^2 = 0$	$x_1 = -\left[\ln\left(2 + \sqrt{3}\right) + \beta\right]/\gamma$	$\frac{\delta^2 y}{\delta x^2} = 0$ or maximum acceleration	SPS_1
	$x_2 = -\left[\ln\left(2 - \sqrt{3}\right) + \beta\right]/\gamma$	$\frac{\delta^2 y}{\delta x^2} = 0$ or maximum deceleration	FPS_1
$\frac{\delta^4 y}{\delta x^4} = 0 \Rightarrow$ $-1 + 11\exp(-\beta - \gamma x) - 11(\exp(-\beta - \gamma x))^2 + (\exp(-\beta - \gamma x))^3 = 0$	$x_1 = -\left[\ln\left(5 + 2\sqrt{6}\right) + \beta\right]/\gamma$	1st inflexion point (ascending)	SPS_2
	$x_2 = -\beta/\gamma$	2nd inflexion point (descending)	IP or MPE
	$x_3 = -\left[\ln\left(5 - 2\sqrt{6}\right) + \beta\right]/\gamma$	3rd inflexion point (ascending)	FPS_2

SPS start of pollen season, 2 metrics; *MPE* maximum pollen emission or inflexion point; *FPS* final of pollen season, 2 metrics

the logistic model occurs (Table 1): start of the pollen season (SPS), maximum pollen emission (IP or MPE) and final of pollen season (FPS). These times are inferred by the second derivative ($^{\delta^2 y}/_{\delta x^2}$) function local minima, maxima and inflexion points (2 ascending and 1 descending), which correspond to the zeros of the third and fourth derivatives. Therefore, for each SPS and FPS, two metrics were extracted; one matching the zeros of third derivatives (SPS_1 and FPS_1) and the other the zeros of fourth derivatives (SPS_2 and FPS_2). Table 1 presents the algorithms used to calculate x_t values of the logistic model that make the third and fourth derivatives equal to zero and the corresponding airborne pollen metrics. The graphical representation of the relationship between the airborne pollen metrics (SPS, IP or MPE and FPS) and the changes of the second derivatives function are presented in the Fig. 2.

Outside the period between the 1st and last inflexion points of the second derivative function, the changes in y_t are very small, and apparently without practical interest for the phenology dynamics.

The statistic analyses presented in the next section were made to decide about the accuracy and precision of the referred metrics to explain the field phenological stages.

2.4 Data analysis

In order to define the most appropriated airborne pollen metrics (SPS, MPE and FF) to represent the phenological observation dates (SF, MF and FF), the following set of comparisons was made in both regions:

- SF was compared with SPS_1, MPE and SPS_2;
- MF was compared with SPS_1, SPS_2, MPE and FPS_2;
- FF was compared with SPS_2 and FPS_2.

No single parameter is sufficient to adequately assess the performance when comparing observed and model-predicted values. Nevertheless, each criterion highlighted particular aspects of comparison. In this context, several statistical procedures were used to make comparisons between airborne metrics and observed phenological data:

- The pairs from observed (phenophases) and model-predicted (metrics) dates were plotted, and a line of identity or a concordance line was drawn through the origin at 45°. In this regression line, the model-predicted values were plotted in the *x*-axis because they are deterministic with no random variation, whereas the observed values contain natural values.
- A paired *t* test was performed to test the hypothesis of no between-approaches differences. This statistical test checks only whether the mean results are the same, while the (random) differences between measurements can be large even for equal means. In order to avoid this misinterpretation, other complementary statistics tests were used to assess the agreement between approaches.
- The assessment of the between-methods agreement was also quantified with Lin's concordance correlation coefficient—CCC (Lin and Torbeck 1998). Calculations were based on an algorithm that contains both a measure of accuracy (how far the best-fit line deviates from the concordance line) and a measure of precision (how far each observation deviates from the best-fit line). A CCC value equal to 1 represents perfect agreement, and CCC = 0 no agreement at all.

In this work, the level of between-approaches agreement was classified as follows: excellent (CCC 0.81–1.00), substantial (CCC 0.61–0.80), moderate (CCC 0.41–0.60), fair (CCC 0.21–0.40), slight (CCC 0.00–0.20) and poor (CCC < 0.00) (Landis and Koch 1977).

- Methods suggested by Altman and Bland (1971) were applied to the data to evaluated the between-approaches disagreement and the relative contribution of bias and error. The differences between observed phenophases and airborne pollen metrics dates were plotted against their average for visual assessment of bias and error to spot outliers and to see whether there was any tendency for the amount of variation to change with the magnitude of the measurements.
- A model fitting analysis comprising the mean absolute difference (MAD) and root-mean-square error (RMSE) between observed and model predicted values was performed.

3 Results

A descriptive statistics for the observed flowering and airborne pollen metrics dates for both studied regions is presented in Table 2.

The period analysed in VVR (1993–2007) is shorter than the period for Douro region (1992–2011). However, the coefficient of the variation (C.V. %) in both regions is very similar (differences <2 %) for all the variables tested (Table 2), so we can assume that the variances of the samples are homogeneous. Our modelling assumption is that the variances of the different samples are homogeneous and the sample size difference (five observations) is reasonably small not to jeopardise the stability results.

There was a marked annual variability in the mean flowering date among and within regions. The grapevine flowering occurred between May and June, being the start, peak and final metrics dates, consistently

Table 2 Descriptive statistics of grapevine phenological stages and airborne pollen metrics for Douro and Vinho Verdes wine regions

Statistics	Units	Phenological stages				Airborne pollen metrics					
		SF	MF	FF	FF–SF	MPE	SPS_2	FPS_1	SPS_1	FPS_2	FPS_2–SPS_1
Vinhos Verdes region (1993–2007)											
Mean	DOY	148.8	156.4	164.3	15.5	155.8	148.4	163.1	142.9	168.6	25.7
Coef. variation	%	10.7	6.8	6.8	31.1	7.7	8.3	7.5	9.0	7.6	35.6
Maximum	DOY	166.0	174.0	182.0	28.0	168.1	162.5	176.3	159.1	185.8	44.5
Minimum	DOY	122.8	131.3	135.0	10.0	123.1	115.5	130.7	109.8	136.4	14.7
Douro region (1992–2011)											
Mean	DOY	–	140.8	145.5	–	142.0	135.3	147.8	130.7	152.4	21.0
Coef. variation	%	–	7.1	7.1	–	7.2	7.3	7.4	7.4	7.7	37.4
Maximum	DOY	–	155.8	162.3	–	154.6	148.7	165.4	145.4	173.3	30.2
Minimum	DOY	–	112.0	115.0	–	114.6	109.5	119.0	106.0	122.5	12.7

– no data, *SF* start of flowering period, *MF* main flowering period, *FF* final flowering period, *SPS* start of pollen season, *MPE* maximum pollen emission and *FPS* final of pollen season are pollen metrics extracted from the pollen emission model (Table 1)

Table 3 Statistics of pollen emission model adjusted parameters and model fitting over the studied years

Statistics	R^2	Model parameters		
		α	β	γ
Vinhos Verdes region (1993–2007)				
Mean	0.987	76.5	31.4	−0.201
C.V. (%)	0.820	55.8	36.7	35.1
Minimum	0.965	31.0	16.9	−0.103
Maximum	0.995	173.1	49.4	−0.313
Douro region (1992–2012)				
Mean	0.980	273.0	33.2	−0.227
C.V. (%)	0.921	44.8	33.1	32.1
Minimum	0.962	93.9	15.0	−0.105
Maximum	0.994	414.5	57.8	−0.380

earlier in Douro region than in VVR. For Douro, the mean flowering date from phenological observations was the DOY 141 and ranged from the earliest recorded in DOY 112 (1997) to DOY 156 (1993).

The over years mean duration of pollen season in Douro determined by the pollen metrics was 21 days, being 5 days shorter than in VVR. The annual fluctuations in the duration of the main pollen period indicate the overall climate in those periods. VVR is characterised by interannual variation in the main pollen period that extends from 15 days (2004) to 45 (1998) days, being the region that has the highest precipitation.

Table 3 shows the statistics of the model parameters adjusted for both regions. The logistic model accounts for more than 97 % of variation in accumulated airborne pollen model.

The model's parameters estimated for both regions present a great variability among years. The larger differences between regions were observed for the logistic model parameter α (4.5 times more in VVR), reflecting the differences in climate conditions and particularly the location of the pollen traps (distance and height) relatively to vegetation surrounding. The other model parameters (β, γ) presented similar statistics in both regions (Table 3).

Table 4 shows a set of diagnostic tests to confirm the most appropriated metrics to be used for each field observation of flowering dynamics.

The pollen-derived flowering metrics for both regions was found to be significantly correlated with flowering dates (SF, MF and FF) observed at field level. According the statistical tests presented in the Table 4, the most appropriated airborne pollen metrics to represent the timing of SF, MF and FF field measurements in both regions are, respectively, the SPS_2, MPE and FPS_1.

The mean absolute between-approaches difference indicates that the logistic model inflection point (MPE) and the corresponding 2nd to 4th derivatives (SPF_2 and FPS_1) would be 3 days accurate for the over year start (data only available for VVR) and peak flowering dates and 5 days accurate in explaining the

Table 4 Statistics for each pair of observed grapevine phenological stages and model-predicted pollen metrics in both studied regions

Statistics	SF			MF				FF	
	MPE	SPS_2	SPS_1	MPE	SPS_2	FPS_1	SPS_1	FPS_1	FPS_2
Vinhos Verdes region (VVR)									
MAD	7.1	*2.7*	6.1	*3.2*	8.2	7.4	13.8	*4.6*	6.5
RMSE	8.1	*3.0*	6.7	*4.0*	8.8	8.7	14.2	*5.2*	7.6
ICC_v	0.772	*0.964*	0.847	*0.941*	0.751	0.736	0.545	*0.895*	0.798
ICC_p	Substancial	*Excellent*	Excellent	*Excellent*	Substantial	Substantial	Moderate	*Excellent*	Substantial
t test *p* value	0.000	*0.605*	0.000	*0.539*	0.001	0.001	0.000	*0.404*	0.028
Slope[a]	1.0468	*0.9978*	0.9616	*0.9959*	0.9492	1.0426	0.9146	*0.9928*	1.05258
R^{2a}	0.8723	*0.9374*	0.9202	0.8824	*0.8992*	0.7733	0.8559	*0.8152*	0.7403
Douro region									
MAD	–	–	–	*2.8*	5.3	7.1	9.8	*4.3*	6.7
RMSE	–	–	–	*3.4*	6.5	8.3	10.7	*5.1*	8.3
ICC_v	–	–	–	*0.940*	0.789	0.731	0.585	*0.884*	0.744
ICC_Class	–	–	–	*Excellent*	Substantial	Substantial	Moderate	*Excellent*	Substantial
t test, *p* value	–	–	–	*0.322*	0.000	0.000	0.000	*0.173*	0.000
Slope[a]	–	–	–	*1.0089*	0.9623	1.0498	0.9299	*1.0106*	1.0418
R^{2a}	–	–	–	*0.8949*	0.8419	0.8216	0.7951	*0.7933*	0.7528

MAD mean absolute difference, *RMSE* root-mean-square error, *CCC* concordance correlation coefficient

[a] Slope and R^2 of the regression trough zero. Best results are in italics

final of flowering compared with that observed in surrounding fields in both regions.

Testing of the hypothesis of zero means or no bias showed that observed approach gives results that are not significantly different from the selected airborne metrics. The regression through zero presents high R^2 (>0.80) and a slope close to 1. For all pairs of comparisons, the CCC is always rated as excellent.

The differences between each pair of phenological and best derived pollen metrics are always lower than 10 days (Fig. 3). For the VVR with the 14 annual records, the between-approaches differences in 93 % (for the SF-SPS_2) and 86 % (MF and MPE) were below 5 days. For the final of the flowering period, 36 % of the cases present between-approaches differences between 5 and 10 days. The between-approaches differences for the final of the flowering period in 37 % of the cases were between 5 and 10 days (Fig. 3).

In Douro region, for the studied period 1992 to 2011 with 19 annual records (lack of data for 2010), descriptive statistics show, for the timing of the main flowering period, that 84 % of the cases had between-approaches differences below 5 days and only in three observations occurred differences higher than 5 days but lower than 10 days.

Differences between each pair of phenological observation and model-predicted values of flowering phenophases plotted against corresponding mean (Fig. 4) spread on both sides of the "0" line. However, it is noticeable that a great number of observed MF (6/13) and FF (8/11) differences in Douro are below the "0" line, suggesting a tendency for the observed phenological approach to provide early dates.

In VVR, the SF and FF present similar number of observations on both sides of the "0" line, but in 9/5 of the years, the FPS occurred earlier than the observed FF. However, the time span between these events was lower than 5 days.

4 Discussion

As stated by Scheifinger et al. (2013), there is an increased importance of a more comprehensive understanding of the relationship between airborne pollen time series and the dynamic of the surrounding vegetation in supporting simulate regional pollen

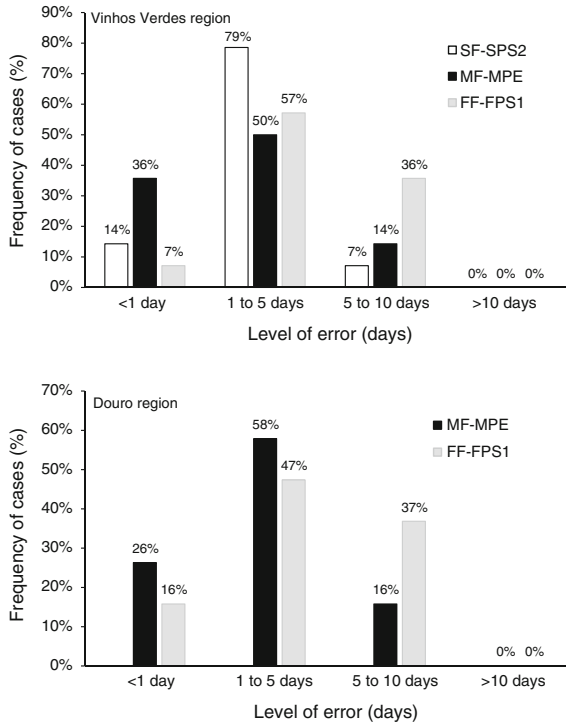

Fig. 3 Frequency levels of errors between each pair of phenological and derived pollen metrics

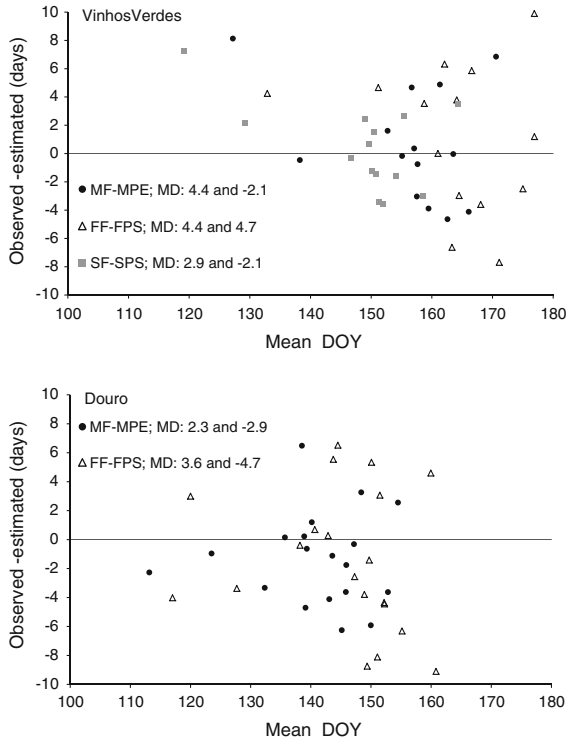

Fig. 4 Disagreement between dates (days) of each pair of phenological observations and pollen metrics (SF–SPS, MF–MPE and FF–FPS) plotted against their average mean dates (DOY) in both studied region. MD is the mean difference of positive and negative cases, respectively

dispersal within the framework of sophisticated regional air-quality models. In this context, modelling efforts have been made to forecast the pollen metrics via meteorological data and/or field observation of the flowering phenophase. These models are either based on simple regression of phenological and aerobiological observations (e.g. Jato et al. 2007; Kasprzyk and Walanus 2010), or they generate daily pools of pollen available for release (emission potentials) into atmosphere using physical principles of transport and meteorological parameters such temperature, precipitation and wind (Siljamo et al. 2008b; Martin et al. 2009; Zhang et al. 2013; Brighetti et al. 2014).

To our knowledge, there is not yet a well-established method for treating pollen emissions in regional forecasting models. However, sensitivity studies suggest that the estimation of the pollen source is a major factor of uncertainty for simulated airborne pollen time series (Zhang et al. 2013; Scheifinger et al. 2013). Therefore, as outlined by Estrella et al. (2006), these regional forecasting models might be restricted in its practical application, if most of the airborne pollen collected on the trap does not originate from the surrounding vegetation. Hence, the airborne metrics extracted by the logistic model, herein presented as prediction tool of observed phenology, could be a significant contribution towards improving the accuracy of simulate regional pollen dispersal.

The results show that the logistic regression model fits well the airborne pollen results of the serial filters exposed during the *Vitis* flowering period in two regions in northern Portugal. However, the proposed logistic model should be obviously open to further confirmation and refinement with a view to providing a more universal application in the future, with regard not only to the tested taxa in Portugal environment but also to other pollen grains and particular features of the sampling site involved.

The pollen metrics extracted by the logistic pollen emission model are an expedient and reliable mean to estimate the beginning and the final of pollen season that also allows to avoid the contribution from pollen deposition and recirculation as well as from the

transport from long distances. One important factor in crop forecasting models is the knowledge of the real amount of pollen that will be directly involved in the onset of local pollination. Hence, our results may be also used to improve the accuracy of these forecast models through the accurate definition of the quantity of regional pollen used.

We consider the proposed method useful for comparing the beginning and duration of pollen season among years, but not appropriated to determine the start of pollen season on behalf of allergic airway diseases, because this model can only be used in retrospect. Also, contrary to crop forecasting, the contribution of pollen recirculation and long-distance transport can have important impact on respiratory allergy (Veriankaite et al. 2010).

The logistic model's parameters estimated for both regions presented a great variability among years. Since the vineyard surface was relatively constant over the studied period, these parameters' variability could be related to the number of flowers and climate conditions.

The developed model proved to be accurate and precise in defining the main flowering phenophase of the vineyards surrounding the pollen trap in both regions. Using the phenological observations dataset as the benchmark, airborne pollen-derived metrics data within the same region are compared for year-to-year data. Despite the great differences among regions in terms of biophysical characteristics and the number of observations, each pair of phenological and derived pollen metrics approaches presents similar pattern for the frequency of timing differences in days. Results indicate that between-approaches mean absolute differences were always lower than 5 days for estimating the start, peak and final flowering dates in both regions. The final flowering stage in 37 % of the cases presented between-methods differences of 5–10 days, being the phenophase with higher between-approaches timing differences.

Under the current parameterisation scheme, the model tends to underestimate the timing of MF and FF in Douro region and tends to overestimate the date of FF in VVR. This is presumed to result from the temporal non-alignment between modelled pollen seasons at large scale and observed phenology in small plots or because there are additional *Vitis* pollen in the domain which were not included in the model. However, this tendency should be relativised according the low differences between approaches. The results of field phenology observations were assumed as more accurate than the results measured by the airborne pollen analysis. So the measures of accuracy and precision provided are in relation to this dataset which is known to have its own inaccuracies (close to what was produced here).

The results indicate that the logistic model inflection point would be about 90 % accurate in predicting the main flowering date variability over years, which is strong evidence that the pollen emission model satisfactorily predicts this phenophase. The flowering date marks the transition from vegetative to the reproductive crop physiological process and also the start of fruit development period, a crucial stage for crop modelling and field operations. Moreover, this date is of particular interest since it determines any advance or delay in crop cycle (e.g. Osborne et al. 2000). For example, the date of flowering is important to determine the date of harvest, because there is a constant number of temperature units (°C day) accumulated during the day between flowering and harvest (Cunha et al. 2010).

Often, more important than the actual date of each phenological event is the interval between events, which gives an indication of the overall climate and physiology process during those periods. Long seasons indicate less than ideal climate conditions during the flowering period and/or heterogeneity of flowering dates that can affect negatively the grape quantity. Short intervals between pollen metrics can be associated with optimum conditions for pollen emission, transport and deposition as well as a uniformity of flowering dates.

5 Conclusion

In this work, the airborne pollen metrics of *Vitis* extracted from a logistic model were compared against field measurements of flowering dynamics using a long time series of data. The airborne pollen-derived metrics for Vinhos Verdes and Douro regions were found to be significantly correlated with flowering dates (start, main and final flowering) observed at field level.

The results support the hypothesis that the logistic model fits well the airborne time series from different years and regions. The rate of changes of the logistic

model inferred by derivatives is an expedient and reliable means to achieve airborne pollen metrics and to explain the surrounding vegetation dynamics. Therefore, our approach based on temporal trajectory analysis of modelled airborne time series, capable of separating out changes at different points in time with respect to vegetation dynamic, proved to be adequately flexible to capture these features and the important biophysical and geospatial information contained therein.

While this airborne pollen metric approach of flowering dynamic can only give indications of causal relationships on potential climatic growth and physiological impact, they provide the catalyst for causal hypothesis generation, namely for the pollen metrics crop size and quality interactions, which could be tested where other data sources are available. The quantification of the relative impact of these myriad factors on the flowering dynamics is still a huge challenge for developing strategies for the crop size and quality forecasting, as well as other applications of aerobiology.

Acknowledgments The authors would like to thank Carlos Coutinho (Estação de Avisos da Direcção de Agricultura e Pescas do Norte) and J.Pedro Pereira (Subvidouro) for providing the vineyard phenological data used for model validation. We also thank António Teixeira for assisting in the pollen collection.

References

Altman, D. G., & Bland, J. M. (1971). Measurement in medicine: The analysis of method comparison studies. *Statistician, 221*, 850–892.

Andersen, T. B. (1991). A model to predict the beginning of the pollen season. *Grana, 30*(1), 269–275.

Baggiolini, M. (1952). Les stades reperes dans le developpment annuel de la vigne et leur utilization pratique. *Revue romande d'Agriculture et d'Arboriculture, 8*, 4–6.

Brighetti, M. A., Costa, C., Menesatti, P., Antonucci, F., Tripodi, S., & Travaglini, A. (2014). Multivariate statistical forecasting modeling to predict Poaceae pollen critical concentrations by meteoclimatic data. *Aerobiologia, 30*(1), 25–33.

Cambon, G., Ritchie, J. C., & Guinet, P. (1992). Long-distance transport of airborne pollen in southern Ontario (Canada). *Canadian Journal of Botany-Revue Canadienne De Botanique, 70*(11), 2284–2293.

Charalampopoulos, A., Damialis, A., Tsiripidis, I., Mavrommatis, T., Halley, J., & Vokou, D. (2013). Pollen production and circulation patterns along an elevation gradient in Mt Olympos (Greece) National Park. *Aerobiologia, 29*(4), 455–472.

Cour, P. (1974). Nouvelles technique de détection des flux et des retombées polliniques: étude de la sedimentation des pollens et des spores à la surface du sol. *Pollen et Spores XVI, 1*, 103–141.

Cristofori, A., Cristofolini, F., & Gottardini, E. (2010). Twenty years of aerobiological monitoring in Trentino (Italy): Assessment and evaluation of airborne pollen variability. *Aerobiologia, 26*(3), 253–261.

Cunha, M., Abreu, I., Pinto, P., & Castro, R. (2003). Airborne pollen samples for early-season estimates of wine production in a Mediterranean climate of Northern Portugal. *American Journal of Enology and Viticulture, 54*(3), 189–194.

Cunha, M., Marcal, A. R. S., & Silva, L. (2010). Very early prediction of wine yield based on satellite data from VEGETATION. *International Journal of Remote Sensing, 31*(12), 3125–3142.

Davies, R. R., & Smith, L. P. (1973). Forecasting the start and severity of the hayfever season. *Clinical Allergy, 4*, 95–108.

Driessen, M. N. B. M., van Herpen, R. M. A., Moelands, R. P. M., & Spieksma, F. T. M. (1989). Prediction of the start of the grass pollen season for the western part of the Netherlands. *Grana, 28*(1), 37–44.

Duhl, T. R., Zhang, R., Guenther, A., Chung, S. H., Salam, M. T., House, J. M., et al. (2013). The simulator of the timing and magnitude of pollen season (STaMPS) model: A pollen production model for regional emission and transport modeling. *Geoscientific Model Development Discussions, 6*(2), 2325–2368.

Emberlin, J., Jaeger, S., Dominguez-Vilches, E., Soldevilla, C., Hodal, L., Mandrioli, P., et al. (2000). Temporal and geographical variations in grass pollen seasons in areas of Western Europe: An analysis of season dates at sites of the European pollen information system. *Aerobiologia, 16*(3–4), 373–379.

Estrella, N., Menzel, A., Krämer, U., & Behrendt, H. (2006). Integration of flowering dates in phenology and pollen counts in aerobiology: Analysis of their spatial and temporal coherence in Germany (1992–1999). *International Journal of Biometeorology, 51*, 49–59.

Feher, Z., & JaraiKomlodi, M. (1997). An examination of the main characteristics of the pollen seasons in Budapest, Hungary (1991–1996). *Grana, 36*(3), 169–174.

Fernández-Llamazares, Á., Belmonte, J., Boada, M., &, Fraixedas, S. (2013a). Airborne pollen records and their potential applications to the conservation of biodiversity. *Aerobiologia*, *30*(2), 111–122.

Fernández-Llamazares Á., Belmonte J., Delgado R., Linares C. (2013b) A statistical approach to bioclimatic trend detection in the airborne pollen records of Catalonia (NE Spain). *International Journal of Biometeorology*, *58*(3), 371–382.

Galán, C., Emberlin, J., Domínguez, E., Bryant, R. H., & Villamandos, F. (1995). A comparative analysis of daily variations in the Gramineae pollen counts at Córdoba, Spain and London, UK. *Grana, 34*, 189–198.

Giorato, M., Lorenzoni, F., Bordin, A., De Biasi, G., Gemignani, C., Schiappoli, M., et al. (2000). Airborne allergenic pollens in Padua: 1991–1996. *Aerobiologia, 16*, 453–454.

Helbig, N., Vogel, B., Vogel, H., & Fiedler, F. (2004). Numerical modelling of pollen dispersion on the regional scale. *Aerobiologia, 3*, 3–19.

Jarosz, N., Loubet, B., & Huber, L. (2004). Modelling airborne concentration and deposition rate of maize pollen. *Atmospheric Environment, 38*(33), 5555–5566.

Jato, V., Rodríguez-Rajo, F. J., & Aira, M. J. (2007). Use of phenological and pollen-production data for interpreting atmospheric birch pollen curves. *Annals of Agricultural and Environmental Medicine, 14*(2), 271–280.

Kasprzyk, I. (2003). Flowering phenology and airborne pollen grains of chosen tree taxa in Rzeszów (SE Poland). *Aerobiologia, 19*, 113–120.

Kasprzyk, I., & Walanus, A. (2010). Description of the main Poaceae pollen season using bi-Gaussian curves, and forecasting methods for the start and peak dates for this type of season in Rzeszow and Ostrowiec Sw. (SE Poland). *Journal of environmental monitoring: JEM, 12*(4), 906–916.

Kuparinen, A., Schurr, F., Tackenberg, O., & O'Hara, R. B. (2007). Air-mediated pollen flow from genetically modified to conventional crops. *Ecological Applications, 17*(2), 431–440.

Landis, J. R., & Koch, G. G. (1977). Measurement of observer agreement for categorical data. *Biometrics, 33*(1), 159–174.

Lejoly-Gabriel, M., & Leuschner, M. R. (1983). Comparison of airborne pollen at Louvain-La-Neuve Belgium and Basel Switzerland during 1979 and 1980. *Grana, 1*, 59–64.

Lin, L., & Torbeck, L. D. (1998). Coefficient of accuracy and concordance correlation coefficient: New statistics for methods comparison. *PDA Journal of Pharmaceutical Science and Technology, 52*(2), 55–59.

Martin, M. D., Chamecki, M., Brush, G. S., Meneveau, C., & Parlange, M. B. (2009). Pollen clumping and wind dispersal in an invasive angiosperm. *American Journal of Botany, 96*(9), 1703–1711.

Mullenders, W., Dirichx, M., & Haegen, D. V. (1972). La pluie pollinique à Louvain. *Louvain Medical, 91*, 159–176.

Nilsson, S., & Persson, S. (1981). Tree pollen spectra in the stockholm region (sweden), 1973–1980. *Grana, 20*(3), 179–182.

OIV, (2009). *Code des caractères descriptifs des variétés et espèces de Vitis* (2nd ed.). Organisation Internationale de la Vigne et du Vin (OIV).

Orlandi, F., Romano, B., & Fornaciari, M. (2005). Effective pollination period estimation in olive (*Olea europaea* L.): A pollen monitoring application. *Scientia Horticulturae, 105*, 313–318.

Osborne, C. P., Chuine, I., Viner, D., & Woodward, F. I. (2000). Olive phenology as a sensitive indicator of future climatic warming in the Mediterranean. *Plant, Cell and Environment, 23*, 701–710.

Pathirane, L. (1975). Graphical determination of the main pollen season. *Pollen et Spores, 17*, 609–610.

Ribeiro, H., Cunha, M., & Abreu, I. (2007). Definition of the main pollen season using a logistic model. *Annals of Agricultural and Environmental Medicine, 14*(2), 259–264.

Ribeiro, H., Cunha, M., & Abreu, I. (2009). A bioclimatic model for forecasting olive yield. *Journal of Agricultural Science, 147*, 647–656.

Rousseau D. D., Duzer D., Cambon G. V., Jolly D., Poulsen U., Ferrier J., et al. (2003) Long distance transport of pollen to Greenland. *Geophysical Research Letters, 30*(14), 1765.

Ruffaldi, P., & Greffier, F. (1991). Birch (Betula) pollen incidence in France (1987–1990). *Grana, 30*, 248–254.

Sánchez Mesa, J., Smith, M., Emberlin, J., Allitt, U., Caulton, E., & Galan, C. (2003). Characteristics of grass pollen seasons in areas of southern Spain and the United Kingdom. *Aerobiologia, 19*(3–4), 243–250.

Scheifinger, H., Belmonte, J., Buters, J., Celenk, S., Damialis, A., Dechamp, C., et al. (2013). Monitoring, Modelling and Forecasting of the Pollen Season. In M. Sofiev & K.-C. Bergmann (Eds.), *Allergenic pollen* (pp. 71–126). The Netherlands: Springer.

Siljamo, P., Sofiev, M., Ranta, H., Linkosalo, T., Kubin, E., Ahas, R., et al. (2008a). Representativeness of point-wise phenological betula data collected in different parts of Europe. *Global Ecology and Biogeography, 17*(4), 489–502.

Siljamo, P., Sofiev, M., Severova, E., Ranta, H., Kukkonen, J., Polevova, S., et al. (2008b). Sources, impact and exchange of early-spring birch pollen in the Moscow region and Finland. *Aerobiologia, 24*(4), 211–230.

Spieksma, F. T. M., Emberlin, J. C., Hjelmroos, M., Jäger, S., & Leuschner, R. M. (1995). Atmospheric birch (Betula) pollen in Europe: Trends and fluctuations in annual quantities and the starting dates of the seasons. *Grana, 34*(1), 51–57.

Torben, B. A. (1991). A model to predict the beginning of the pollen season. *Grana, 30*, 269–275.

Veriankaite, L., Siljamo, P., Sofiev, M., Sauliene, I., & Kukkonen, J. (2010). Modelling analysis of source regions of long-range transported birch pollen that influences allergenic seasons in Lithuania. *Aerobiologia, 26*(1), 47–62.

Weger, L., Bergmann, K., Rantio-Lehtimäki, A., Dahl, Å., Buters, J., Déchamp, C., et al. (2013). Impact of Pollen. In M. Sofiev & K.-C. Bergmann (Eds.), *Allergenic pollen* (pp. 161–215). The Netherlands: Springer.

Zhang, R., Duhl, T., Salam, M. T., House, J. M., Flagan, R. C., Avol, E. L., et al. (2013). Development of a regional-scale pollen emission and transport modeling framework for investigating the impact of climate change on allergic airway disease. *Biogeosciences Discussions, 10*(3), 3977–4023.